

Silver particles deposited on porous silicon as SERS-active substrate

Changwu Lü (吕长武)¹, Jiajia Wang (王佳佳)¹, Xiaoyi Lü (吕小毅)²,
and Zhenghong Jia (贾振红)^{2*}

¹School of Physical Science and Technology, Xinjiang University, Urumqi 830046, China

²College of Information Science and Engineering, Xinjiang University, Urumqi 830046, China

*Corresponding author: jzhh@xju.edu.cn

Received October 6, 2013; accepted October 19, 2013; posted online March 1, 2014

A simple, low-cost, and high-efficient method is used for the fabrication of surface-enhanced Raman scattering (SERS) substrates. Silver particles deposited on porous silicon are prepared as a highly efficient SERS substrate by direct immersion of porous silicon in silver solution. The SERS measured with rhodamine 6G as a target molecule is affected by the morphology of silver particles on the top of porous silicon layer. The effect of solution concentration, dipping time, and thickness of porous layer on the morphology of silver particle is investigated. Highly efficient SERS spectra are observed for substrates with porous layer thickness of about 3 μm and incubated in the 50 mM AgNO_3 solution for 3 minutes. The SEM images of the substrates show that there are many small Ag particles with the size of a few nanometers among large Ag particles with the size of several microns.

OCIS code: 240.6695, 160.4670, 160.3900, 300.6450.

doi: 10.3788/COL201412.S12401.

Surface-enhanced Raman scattering (SERS) has attracted much attention in recent years due to its excellent performances in amplification of Raman spectrum, which is one of the most promising tools for detection and identification of biological and chemical substances^[1-3]. Recent research demonstrates that the enhancement can be as much as several orders of magnitude and even gives the possibility of single-molecule detection^[4,5]. An enormous amount of effort has been made in developing new and reliable methods for SERS. It is generally believed that two mechanisms are related to the enhancement of the Raman signal—chemical mechanism and electromagnetic mechanism^[6]. Noble metals such as Au and Ag were extensively studied as SERS-active substrates due to their unique surface plasma resonance features. The earliest used substrate is the roughened metal electrode^[7], and the most commonly used substrates are Au and Ag colloids made by several kinds of chemical methods^[8,9]. However, these traditional substrates have some drawbacks such as low sensitivity, unstable, and difficult to produce, which inspired the interest of researchers to work on new SERS-active substrates^[10].

Recently, porous silicon (PS) appeared to be a promising material for the fabrication of SERS-active substrates, owing to its active and rough surface on which noble metal can be deposited to form a rough metal surface^[11,12]. Direct immersion of PS into silver solution was a simple, efficient method to prepare SERS substrate. By means of this method, silver can be deposited on the surface of PS and self-assembled into different nanostructures under different conditions. The resultant dendritic and feather structures exhibited high efficiency in SERS^[13]. Additionally, several SERS-active substrates were also fabricated on n-type and p-type silicon^[14-16].

Our previous work^[16] has made an efficient SERS substrate on n-type PS with the pore size $\sim 1 \mu\text{m}$. In this article, highly efficient SERS substrates were synthesized

based on Ag deposited on p⁺-type mesoporous silicon by a simple but efficient method and has potential application in biosensors. The surface morphology of Ag particles deposited on PS shows some interesting characteristics that may contribute to the high efficiency in SERS. The relation between the deposition condition and the morphology of Ag particles is studied.

Silicon wafers were purchased from the Tianjin Semiconductor Technology Research Institute. Rhodamine 6G (R6G) (analytical reagent) and AgNO_3 (analytical reagent) were purchased from Aladdin Shanghai, China. Scanning electron microscopy images of Ag/PS substrates were obtained by a ZEISS SUPRA 55 VP (Zeiss SMT, Germany) field emission electron microscope (FESM). Raman spectra of R6G were obtained by means of a SENTERRA micro-Raman spectrophotometer (Bruker, Germany) equipped with a cooled CCD camera. A 50 \times objective was used to focus the laser beam on the sample and to collect scattered light from the samples. We illuminated the substrate by means of a focused laser beam with a wavelength of 532 nm, excitation power of 50 mW, and a spot size of 25 \times 1000 μm .

The Si wafers were highly B-doped p⁺-type silicon, 1–3 m Ω /cm, <100>-orientation. The wafer was cut into 1-cm² squares and cleaned with ultrasonic in a solution of acetone, alcohol, and deionized water for 10 minutes successively. The etching process was performed at room temperature in a solution composed by HF (48%) and ethanol in a volume ratio of 1:1. An anodic current density of 60 mA/cm² for 1 minute was applied to fabricate a mesoporous layer with the thickness around 3 μm . Then, the substrates were cleaned with deionized water and dried at room temperature in the air.

Freshly etched PS samples were immersed in aqueous AgNO_3 solution at room temperature for 60, 120, and 180 s, respectively, and rinsed thoroughly with deionized water and then dried in the air. This direct

immersing method for fabricating SERS substrates has some merits such as simplicity, low cost, and high efficiency. The well-dispersed Ag particles were obtained, and the size of these Ag particles is in the range of 10 nm–5 μm , which was dependent on the dipping time and salt concentration. Two concentrations of 10 mM and 50 mM were used in the experiment. We can find that Ag particles formed in the solution with a high concentration had larger size than that in the solution with low concentration under the same dipping time and other conditions, for instance, the thickness of the PS sample. After that, the Ag/PS substrates were cut into two parts, one part was used for morphology scanning and another part for SERS measurement. Next step, the substrates were incubated in R6G solution for 2 hours and then dried in the air. The concentration of the solution was 10^{-6}M , a very low concentration for detection with routine tools. R6G was chosen as our analyte because it has been well characterized by SERS^[17].

Immersion of PS in AgNO_3 solutions is an effective method to synthesize Ag particles through a redox process involving Ag^+ with the hydrides covered surface. The PS samples were etched on p⁺-type silicon. Homogeneous mesopores with an average pore dimension $\sim 15\pm 5$ nm were shown in Fig. 1(c). The nanopores supply a high density of suitable nucleation sites for the particle growth. Fig. 1 shows Ag particles obtained on the PS surface with different magnifications, where the PS sample was etched with the current density of 60 mA/s for 1 minute (thickness about 3 μm).

Then, it was dipped in 50 mM AgNO_3 solution for 3 minutes. Images indicate that the Ag particles grew into different shapes and sizes, from dozens of nanometers to several micrometers. From Fig. 1(b), we can see that there are many pores that are not covered by Ag particles and many small Ag particles with the size of a few nanometers among large Ag particles. This dispersion of Ag particles produces efficient SERS, which was shown by SERS spectra caused by “hot spots” effect^[18].

It is well known that the etched time affects the thickness of the PS and then the PS with different thickness affects the morphology of Ag particles. Figure 2(a) gives the cross-section of Ag/PS substrate with the thickness about 13 μm . The PS sample was etched with the same current for 5 minutes and then also dipped into 50 mM AgNO_3 solution for 3 minutes. Figure 2(b) shows the detail of the cross-section morphology. The dendritic porous layer can be seen, and no Ag particles can be found because the reduction of silver particles on the surface seemed to be fast enough to diffusion of the ions into the pores. Figure 2(c) presents a detail of interface between Ag particles and the porous layer. The Ag particles almost cover the PS in the image range, and there is no gap or pores on the surface compared with Fig. 1. This kind of morphology leads to the decrease in intensity of Raman scattering because the Ag particles are too close that almost like an Ag film covered the surface of porous layer. The effect of PS thickness on the morphology of the Ag particles is examined by SERS spectra of R6G as shown in Fig. 3.

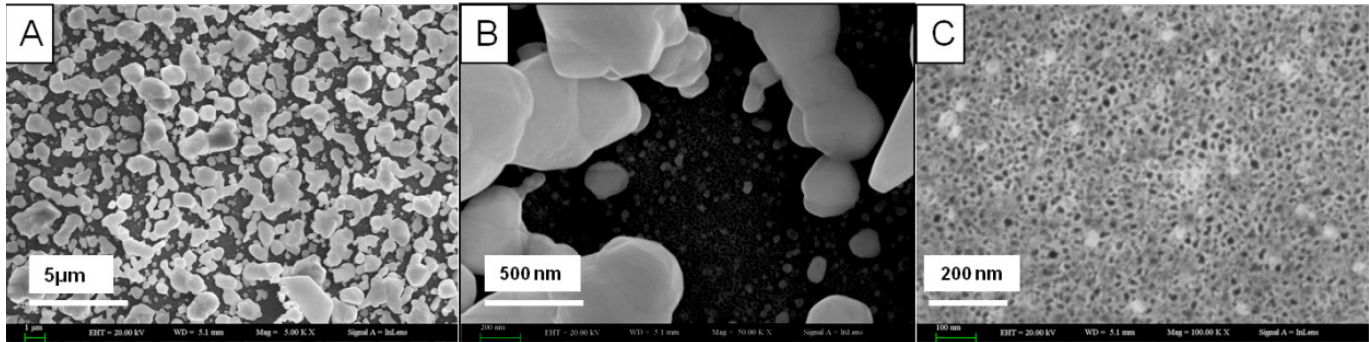


Fig. 1. SEM images of Ag particles obtained by immersion of PS in AgNO_3 solution for 3 minutes, the concentration of AgNO_3 solution was 50 mM. (a) Magnification=5K \times , (b) magnification = 50K \times , (c) magnification=100K \times .

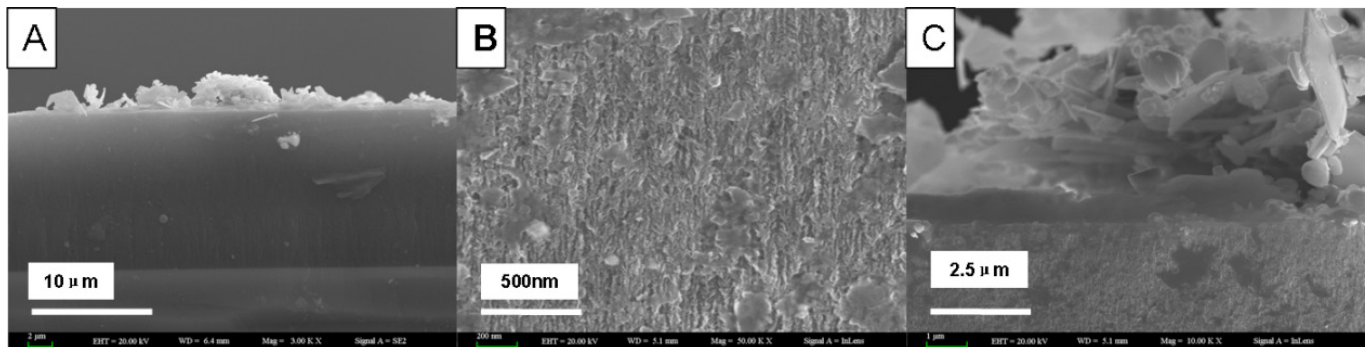


Fig. 2. SERS substrates obtained by immersion of PS (thickness about 13 μm) in AgNO_3 solution for 3 minutes. (a) Cross-section at a large scale, (b) detail in porous layer, and (c) detail at the interface of Ag particles and porous layer.

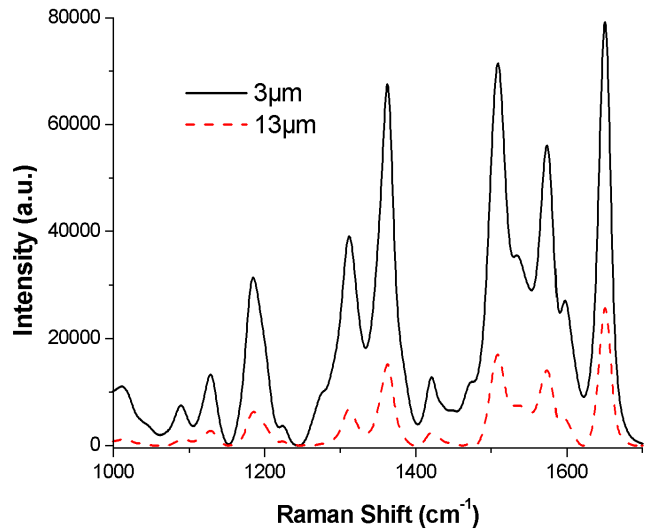


Fig. 3. SERS spectra of R6G for PS immersed in 50 mM AgNO_3 for 3 minutes. The PS samples were etched with the current density of $60\text{mA}/\text{cm}^2$ for 1 minute (thickness about $3\ \mu\text{m}$) and for 5 minute (thickness about $13\ \mu\text{m}$).

The SERS performance is much more better for a thickness about $3\ \mu\text{m}$ than a thickness about $13\ \mu\text{m}$ under the condition that dipping into 50 mM AgNO_3 solution for 3 minutes.

The morphology of the Ag particles is strictly dependent on the concentration of AgNO_3 solution used for the synthesis, the thickness of PS and the dipping time. The effect of concentration of AgNO_3 on the morphology of the Ag particles is examined by SERS spectra of R6G as shown in Fig. 4. A high concentration of 50 mM and a low one of 10mM for AgNO_3 concentration were used in our experiment. The PS samples etched by the same conditions were immersed in the high and low solution, respectively, for the same time (3 minutes). An obvious distinction in the intensity of Raman scattering can be observed in Fig. 4. For the efficiency of SERS is closely related to morphology of Ag

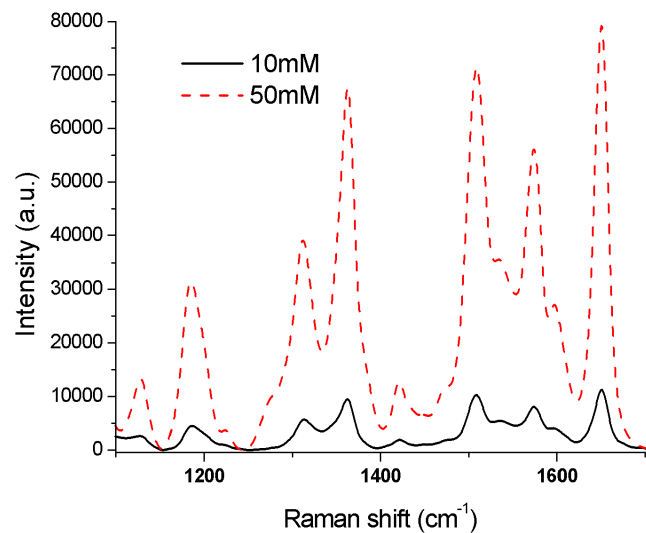


Fig. 4. SERS spectra of R6G for PS immersed in 10 mM and 50 mM AgNO_3

particles on the surface of the PS, which is affected by the concentration of AgNO_3 .

In particular, on fixing the salt concentration, the size of Ag particle increases by increasing the dipping time. Fig. 5 shows SERS spectra of 10^{-6} M R6G on Ag/PS substrates with different dipping time (120, 180, and 210s). It is obviously observed that the intensity of Raman scattering increased with the increase of dipping time at first and then decreased. Both the amount and the size of Ag particles increased with the dipping time. Only single small Ag particles are formed at the beginning, and then they self-assembled into bigger ones with more complicated structures and shapes. However, the large silver particles kept on self-assembling, resulting in a rough Ag film formed on the surface of the PS layer, which has less SERS effect, i.e., the low intensity of Raman scattering.

Based on the above results, it is indicated that the SERS efficiency is strongly dependent on the concentration of solution, thickness, and dipping time. Figure 6 shows the effects of the later two aspects through the SERS spectra of R6G under different conditions. In the same concentration of AgNO_3 solution, Ag is deposited more quickly on the thicker PS samples, and more larger Ag particles are formed for the longer dipping time. In our experiment, the thickness of PS sample is in the range of $2\text{--}6\ \mu\text{m}$ and dipping time varies from 40 to 90 s. An optimal condition corresponding to the thickness about $6\ \mu\text{m}$ and dipping time of 40 s shows the best SERS efficiency among the present experimental conditions.

SERS-active substrates are obtained by the direct immersion of PS samples in AgNO_3 solutions. More efficient SERS spectra are obtained in the present study compared with our previous work^[16]. The SERS is effected by the morphology of the substrate, while it can be controlled by proper fabrication factors such as the dipping time, the concentration of AgNO_3 solution and the thickness of the PS. The highly efficient substrate has some characteristics in the surface morphology of Ag particle, such as Ag particle sizes between a dozen nanometers to several micrometers and a great amount

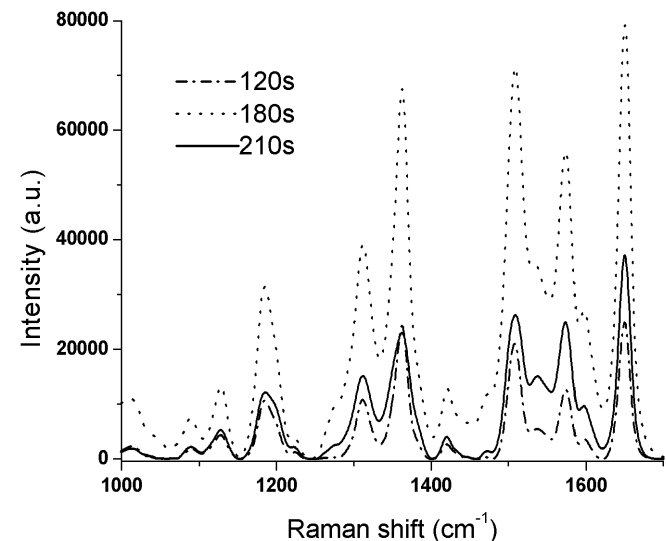


Fig. 5. SERS spectra of R6G for PS immersed in 50 mM AgNO_3 with different dipping times.

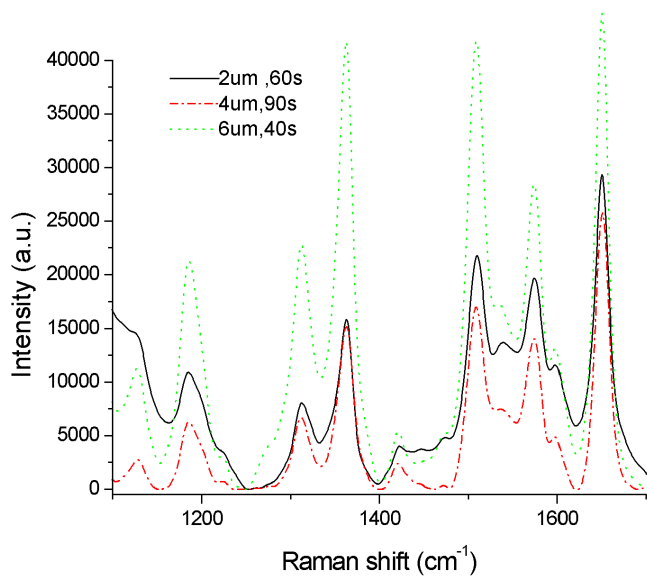


Fig. 6. SERS spectra of R6G for PS with different thickness and dipping times.

of gaps and pores not covered by silver particles. The gaps and pores may absorb small molecule targets and fix them in between Ag particles, thus resulting in a better SERS detection. This kind of morphology can be obtained by optimizing the preparation parameters, such as the concentration of AgNO_3 solution, the dipping time and the thickness of PS. The high-efficient, low-cost and simple SERS-active substrates can be applied in biomolecule detection and have a great potential in the SERS.

This work was supported by the National Science Foundation of China (No. 61265009, 11264038), the Research Fund for the Doctoral Program of Higher Education of

China (No. 20116501110003), and the Xinjiang Science and Technology Project (No. 201291109).

References

1. A. M. Michaels and B. L. Jiang. *J. Phys. Chem. B* **104**, 11965 (2000).
2. T. Vo-Dinh, L. R. Allain, D. L. Stokes. *J. Raman Spectrosc.* **33**, 511 (2002).
3. L. Shupeng, Z. Hongfei, Chen Na, C. Zhenyi, H. Ling. *Chinese J. Lasers* **39**, 0504004 (2012).
4. K. Kneipp, Y. Wang, H. Kneipp, L. T. Perelman, I. Itzkan, R. R. Dasari, and M. S. Feld. *Phys. Rev. Lett.* **78**, 1667 (1997).
5. L. Juqiang, R. Qiuyong, C. Guannan, F. Shangyuan, L. Buhong, C. Rong. *Laser & Optoelectronics Progress* **50**, 080020 (2013).
6. M. Moskovits. *J. Raman Spectrosc.* **36**, 485 (2005).
7. M. Fleischmann, P. J. Hendra, A. J. McQuillan. *Chem. Phys. Lett.* **26**, 163 (1974).
8. K. Kneipp, H. Kneipp, G. Deinum, I. Itzkan, R. R. Dasari, M. S. Feld. *Appl. Spectrosc.* **52**, 175 (1998).
9. M. Futamata, Y. Maruyama, M. Ishikawa. *Vibrational Spectrosc.* **30**, 17 (2002).
10. Z. Jie, C. Yulin, Z. Yong. *Chinese J. Lasers* **39**, 1115001 (2012).
11. S. Chan, S. Kwon, T. W. Koo, L. P. Lee, A. A. Berlin. *Adv. Mater.* **15**, 1595 (2003).
12. R. Miyagawa, K. Fukami, T. Sakka, Y. H. Ogata. *Physica Status Solidi (A)* **208**, 1471 (2011).
13. H. Lin, J. Mock, D. Smith, T. Gao, M. J. Sailor. *J. Phys. Chem. B* **108**, 11654 (2004).
14. A. Y. Panarin, S. N. Terekhov, K. I. Kholostov, V. P. Bondarenko. *Appl. Surface Sci.* **256**, 6969 (2010).
15. L. Zeiri, K. Rechav, Z. E. Porat, Y. Zeiri. *Appl. Spectrosc.* **66**, 294 (2012).
16. H. Zhang, X. Lü, Changwu Lü, Z. Jia. *Opt. Eng.* **51**, 099003 (2012).
17. S. Shim, C. M. Stuart, R. A. Mathies. *Chem. Phys. Chem.* **9**, 697 (2008).
18. J. P. Camden, J. A. Dieringer, Y. Wang, D. J. Masiello, L. D. Marks, G. C. Schatz, and R. P. Van Duyne, *J. Am. Chem. Soc.* **130**, 12616 (2008).